

Liquid Crystals and Phase Equilibria Binary Bile Salt-Water Systems

Eduardo F. Marques,^{*,†,‡} Håkan Edlund,[§] Camillo La Mesa,^{||} and Ali Khan[†]

Physical Chemistry 1, Center for Chemistry and Chemical Engineering, P.O. Box 124, Lund University, Lund SE-221 00, Sweden; Departamento de Química, Universidade de Coimbra, 3049 Coimbra, Portugal; Department of Chemistry and Process Technology, Chemistry, Mid Sweden University, SE-851 70 Sundsvall, Sweden; and Dipartimento de Química, Università degli Studi "La Sapienza", p.le Aldo Moro 5, 00185 Roma, Italy

Received September 28, 1999. In Final Form: February 16, 2000

The phase behavior of several binary sodium bile salt-water systems is investigated over the entire concentration range, with emphasis on concentrated regions beyond the isotropic solution phase. The studied bile acid salts comprise the free salt sodium deoxycholate (SDC), the taurine conjugates sodium taurocholate (STC), sodium taurodeoxycholate (STDC), and sodium taurochenodeoxycholate (STCDC) and the glycine conjugate sodium glycodeoxycholate (SGDC). A combination of classical techniques is used, including phase diagram determination, polarizing microscopy, ²H NMR, and small-angle X-ray scattering (SAXS). The aggregation behavior in the isotropic micellar solutions of STC and STDC is also investigated by pulsed-field gradient NMR self-diffusion. The optical textures and the data from SAXS and ²H NMR clearly point to the formation of hexagonal liquid crystals, possibly of the reverse type, beyond the micellar solution for all the bile salts. Several unusual kinetic effects, such as very slow equilibration times and the formation of transient spherulitic crystals in biphasic regions, are observed. The phase diagrams and structural data are qualitatively discussed in terms of the molecular structure and solubility of the different salts. The formation of lyotropic liquid crystals by bile salts, which has remained unknown for decades, is clearly demonstrated in this work.

1. Introduction

The bile acid salts, or simply bile salts, are amphiphilic molecules of a different kind. They are comparable to common surfactants in that they are surface-active and self-associate in water into micellar-like aggregates.^{1–3} Nonetheless, their association is of low cooperativity, and this is manifested by relatively poorly defined critical micelle concentrations (cmcs). Such amphiphilic properties are enough to render them a fundamental role in the human body,^{4–6} where they occur in the bile produced by the liver and stored in the gallbladder. They act as a solubilizer for lecithin and cholesterol, forming mixed micelles with these otherwise insoluble lipids and thus assisting their excretion from the body. Not least, they form mixed micelles with fatty acids and monoglycerides, the two water-insoluble main products of fat digestion, and promote their absorption by the membrane of intestinal cells.

The peculiarity of bile salts as surface-active agents is directly linked to their molecular structure. The latter differs from that of common surfactants, for which there is a clear-cut separation between the polar (hydrophilic headgroup) and nonpolar regions (typically, flexible alkyl chains). The bile salts are derived from cholic acid, and so, their hydrophobic part consists of a rigid, nonplanar,

steroid fused-ring system. The ring contains from one to three hydroxyl (OH) groups, which means that small hydrophilic groups are present in the hydrophobic moiety. In the cholic acid salt and its conjugates, the OH groups lie in the same side of the ring, so the latter bears both a polar and a nonpolar side (Figure 1). The rigidity and the two-faced character of the ring imply that the packing of the amphiphiles into micelles or other supramolecular structures does not follow the conventional picture for surfactant aggregates. At the cmc, the bile salt molecules are believed to pack in a back-to-back way into roughly spherical micelles of small aggregation numbers, typically $N_{\text{agg}} = 4–10$.^{2,7,8} The values of N_{agg} increase significantly as a function of added electrolyte for some of the bile salts, in accordance with typical surfactant behavior. In some systems, such as the sodium deoxycholate–water system, fibers or long rodlike structures are drawn from concentrated micellar solutions, and on the basis of X-ray data, a helical structure for the fibers has been proposed.^{9–14}

The structural and interfacial properties of the isotropic solution in several binary bile salt-water systems have been studied for a few decades.^{1,2,7,15–19} There are also

(7) Mazer, N. A.; Carey, M. C.; Kwasnick, R. F.; Benedek, G. B. *Biochemistry* **1979**, *18*, 3064.

(8) Kratochvil, J. P. *Adv. Colloid Interface Sci.* **1986**, *26*, 131.

(9) Rich, A.; Blow, D. M. *Nature (London)* **1958**, *182*, 4776.

(10) Blow, D. M.; Rich, A. *J. Am. Chem. Soc.* **1960**, *82*, 3566.

(11) Giglio, E.; Loreti, S.; Pavel, N. V. *J. Phys. Chem.* **1988**, *92*, 2858.

(12) Briganti, G.; D'Archivio, A. A.; Galantini, L.; Giglio, E. *Langmuir* **1996**, *12*, 1180.

(13) D'Archivio, A. A.; Galantini, L.; Giglio, E.; Jover, A. *Langmuir* **1998**, *14*, 4776.

(14) Bottari, E.; D'Archivio, A. A.; Festa, M. R.; Galantini, L.; Giglio, E. *Langmuir* **1999**, *15*, 2996.

(15) Ekwall, P.; Sjöblom, L. *Acta Chem. Scand.* **1948**, *3*, 1179.

(16) Ekwall, P. *J. Colloid Sci.* **1954**, *8*, 66.

(17) Murata, Y.; Sugihara, G.; Fukushima, K.; Tanaka, M.; Matsushita, K. *J. Phys. Chem.* **1982**, *86*, 4690.

(18) Kratochvil, J. P.; Hsu, W. P.; Kwok, D. I. *Langmuir* **1986**, *2*, 256.

(19) Bottari, E.; Festa, M. R. *Langmuir* **1996**, *12*, 1777.

* E-mail: eduardo.marques@fkem1.lu.se or emarques@ci.uc.pt.

† Center for Chemistry and Chemical Engineering.

‡ Universidade de Coimbra.

§ Mid Sweden University.

|| Università degli Studi "La Sapienza".

(1) Fontell, K. *Kolloid-Z. Z. Polym.* **1971**, *244*, 246.

(2) Carey, M. C.; Small, D. M. *Arch. Intern. Med.* **1972**, *130*, 506.

(3) Mysels, K. J. *Hepatology* **1984**, *4*, 80S.

(4) Carey, M. C.; Small, D. M. *Am. J. Med.* **1970**, *49*, 590.

(5) Small, D. M. *The Bile Acids*; Nair, P. P., Kritchevsky, D., Eds.; Plenum Press: New York, 1971.

(6) Borgström, B. *Int. Rev. Physiol.* **1977**, *12*, 305.

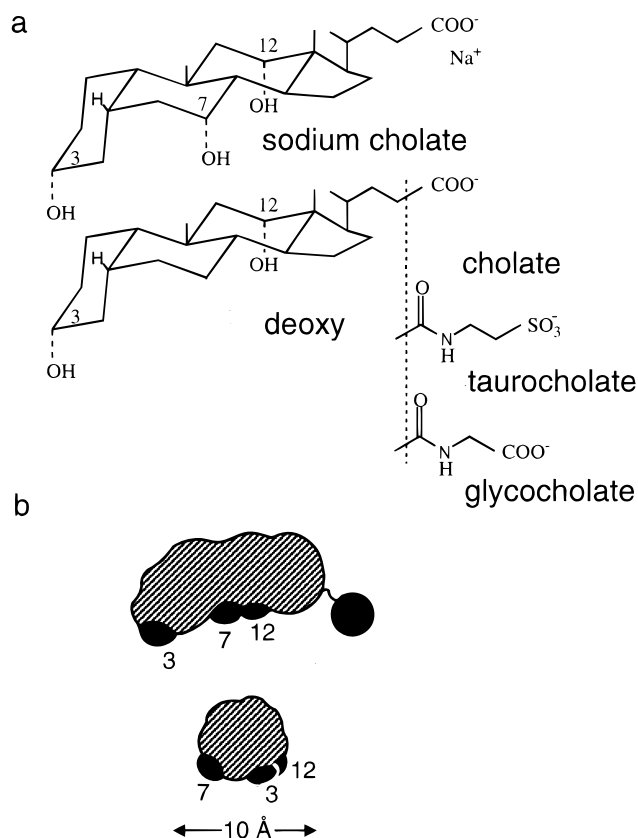


Figure 1. Molecular structure of the bile salts. (a) Sodium cholate ($3\alpha, 7\alpha, 12\alpha$ -trihydroxy- 5β -cholan-24-oic-acid salt) and its deoxycholate derivative, the $3\alpha, 12\alpha$ -dihydroxy salt. The chenodeoxy derivative is the $3\alpha, 7\alpha$ -dihydroxy salt. The structure of the taurine and glycine conjugates is also shown. (b) Longitudinal and transverse view of the cholate molecule, where the relative position of the $3\alpha, 7\alpha$, and 12α OH groups is visible (adapted from Carey and Small.²)

reports on the phase behavior and aggregate structure of mixed systems composed of bile salt–phospholipids^{20,21} and bile salt–single-chained surfactants.^{22–25} While bile salts can be incorporated in a variety of liquid-crystalline (lc) phases in mixed systems, it has been assumed since early studies that they alone do not form liquid-crystalline phases in water. This observation has been acknowledged by most authors as another example of the peculiarity of bile salts. Nonetheless, in a recent report by us, it has been clearly shown by a combination of techniques that, at room temperature, sodium taurodeoxycholate (STDC) forms a wide liquid-crystalline region of hexagonal-like structure.²⁶ It thus appears that the phase behavior of neat bile salts in water, at concentrations higher than the micellar regions, has not been thoroughly investigated. The motivation behind this paper is thus to investigate whether the observation in the STDC system is a singular occurrence or, as can be reasonably expected, if a general pattern of lyotropic liquid-crystal behavior is to be found for bile salts.

(20) Ulmius, J.; Lindblom, G.; Wennerström, H.; Johansson, L. B.-Å.; Fontell, K.; Söderman, O.; Arvidson, G. *Biochemistry* **1982**, *21*, 1553.

(21) Thurmond, R. L.; Lindblom, G.; Brown, M. F. *Biophys. J.* **1991**, *60*, 728.

(22) Barry, B. W.; Gray, G. M. T. *J. Colloid Interface Sci.* **1975**, *52*, 327.

(23) Svård, M.; Schurtenberger, P.; Fontell, K.; Jönsson, B.; Lindman, B. *J. Phys. Chem.* **1988**, *92*, 2261.

(24) Wu, K.; McGown, L. B. *J. Phys. Chem.* **1994**, *98*, 1185.

(25) Swanson-Vethamuthu, M.; Almgren, M.; Bergenstahl, B.; Mukhtar, E. *J. Colloid Interface Sci.* **1996**, *178*, 538.

(26) Edlund, H.; Khan, A.; Mesa, C. L. *Langmuir* **1998**, *14*, 3691.

Human bile is mainly composed of the sodium and potassium salts of the glycine and taurine conjugates of cholic acid and its deoxy and chenodeoxy derivatives. In this paper, we investigate the phase behavior in water of several common bile salts, comprising the sodium salts of the free deoxycholic acid and some of its taurine and glycine conjugate salts (taurocholate, taurodeoxycholate, taurochenodeoxycholate, and glycodeoxycholate). The phase diagrams and the phase structure were obtained by a combination of ocular observations, polarizing microscopy, NMR methods (²H quadrupolar splitting and ¹H self-diffusion), and small-angle X-ray scattering data. Slow kinetics of liquid-crystal formation and phase equilibration seem to be the general rule for the binary systems at high bile concentrations. The assignment of the phases present in the biphasic regions found in some systems is not always straightforward. In a sense, the polymorphic character of the bile salts is also an elusive one. It is perhaps this character that has led some authors in the past to circumvent their lyotropic liquid-crystal formation.

2. Experimental Section

2.1. Materials. The bile acids in the form of sodium salts were purchased from Sigma and used without further purification. D₂O supplied by Dr. Basel, Switzerland, was used in all the samples for the ²H and self-diffusion NMR measurements. The following bile salts were used: sodium deoxycholate (SDC), monohydrate form, >99%; sodium taurocholate (STC), >97%; sodium taurodeoxycholate, 0.5 mol H₂O/mol, >97%; sodium taurochenodeoxycholate (STCDC), high purity; and sodium glycodeoxycholate (SGDC), 1.5 mol H₂O/mol, >98%. The molecular structure for sodium cholate (the free acid form) can be seen in Figure 1a, together with that of the deoxy derivative of the tauro and glyco conjugates. The cholic acid salt has hydroxyl groups in the three carbon positions α C-3, α C-7, and α C-12 (Figure 1a). These three hydroxyl groups and the two hydroxyl groups in the deoxy derivative (α C-3 and α C-12) point to the same side of the steroid ring, giving it one polar and one nonpolar side. The chenodeoxy derivative differs from the deoxy one in that the two OH groups lie in positions α C-3 and α C-7. The relative spatial position of the three carbon atoms is more easily visualized in Figure 1b.

2.2. Sample Preparation and Phase Diagram Determination. The samples were prepared by weight in test tubes which were flame-sealed and thoroughly mixed by repeated centrifugation. They were then allowed to stand at the desired temperature in an oven for equilibration over several weeks. Preliminary studies of the phase behavior involved the inspection of all samples between crossed polaroids in order to check for birefringence. Further assignment of the phase behavior was based on the combined experimental data supplied by polarizing microscopy, ²H NMR, and SAXS. The same techniques were used to delineate phase boundaries.

2.3. Polarized Light Microscopy. Under polarized light, isotropic phases show as a dark background in the microscope, while anisotropic phases show characteristic optical textures.^{27,28} An Axioplan Universal polarizing light microscope (Carl Zeiss), equipped with a highly sensitive SIT C video-camera system and Argus-20 image processor (Hamamatsu Photonics, Japan), was used. The microscope is also equipped with a hot stage operating between -20 and +100 °C.

2.4. Small-Angle X-ray Scattering (SAXS). The measurements were carried out in a Kratky compact small-angle system equipped with a position-sensitive detector, containing 1024 channels of width 53 μ m. A Cu K α radiation of wavelength 1.542 Å was used, and the sample-to-detector distance was 277 mm. The samples for SAXS were prepared in a paste holder between thin mica windows, and the temperature in the sample container was regulated by a Peltier element (accuracy within \pm 0.1 °C). The camera volume was kept under vacuum to minimize air scattering.

(27) Rosevear, F. B. *J. Am. Oil Chem. Soc.* **1954**, *31*, 628.

(28) Rosevear, F. B. *J. Soc. Cosmet. Chem.* **1968**, *19*, 581.

2.5. ^2H (Deuterium) Quadrupolar Splitting NMR. The method was carried out by using deuterated water (D_2O) in the samples. The ^2H nucleus has a spin quantum number $I=1$, and therefore, it possesses an electric quadrupole moment. In anisotropic liquid-crystalline phases (e.g., hexagonal and lamellar phases), the interaction of the quadrupole moment with nearby electric field gradients gives rise to a ^2H splitting. In isotropic phases (solutions and cubic phases), the interaction is averaged to zero by the rapid isotropic molecular motions, and thus, a single signal results. In multiphase samples, due to slow deuteron exchange between the phases, the resultant ^2H spectrum is a superposition of the spectra of the individual phases. The technique is thus effective in delineating multiphase regions, involving two or more liquid-crystalline phases (often difficult to macroscopically separate) or small amounts of isotropic phases.^{29–31} The magnitude of the ^2H quadrupolar splittings (Δ), measured as peak-to-peak separations in hertz, depends on the degree of anisotropy of the phase. For a nonoriented liquid-crystalline sample, Δ is given by

$$\Delta = \frac{3}{4} \sum p_i \nu_Q^i S_i \quad (1)$$

where p_i is the fraction of deuterons in site i , characterized by the order parameter S_i and the effective quadrupolar coupling constant ν_Q^i . In surfactant–water systems, water associates to the headgroups of the amphiphilic molecules which are organized into different aggregate structures. A two-site model can thus be applied with free and bound water molecules. Assuming a fast exchange between the sites and $\Delta = 0$ for free water, the observed Δ for a given liquid-crystalline phase is related to the molar ratio between surfactant and water through

$$\Delta = |\nu_Q S| n \frac{X_S}{X_W} \quad (2)$$

where X_S and X_W are, respectively, the molar fractions of surfactant and water, n is the average hydration number of the surfactant, and ν_Q is the deuteron quadrupolar coupling constant.

The ^2H spectra were recorded at a resonance frequency of 41.45 MHz in a JEOL FX 270 superconducting pulsed FT NMR spectrometer. A variable-temperature control unit was used to regulate the temperature of the air flow in which the samples were located. After being rapidly transferred to the thermostated NMR probe, the samples were kept there for a sufficiently long period to avoid a temperature gradient before the spectra were recorded. The recordings were repeated over several weeks until no changes in the pattern of the spectra were observed.

2.6. Pulsed Field Gradient (PFG) NMR Self-Diffusion. The PFG technique for measuring self-diffusion coefficients is based on a combination of a sequence of radio frequency (rf) pulses and magnetic field gradient pulses.^{32,33} In this method, one monitors the attenuation of a ^1H spin echo resulting from the dephasing of the nuclear spins due to the combined effect of translational motion of the spins and the imposition of the gradient pulses. The self-diffusion coefficient of the diffusing spins can thus be directly extracted from the echo attenuation. The typical PFG sequence is based on the Hahn spin echo and is known as the Stejskal–Tanner experiment. It consists of two rf pulses (a 90° and 180° pulse) and two gradient pulses with time duration δ and separation Δ between their leading edges, placed on either side of the 180° rf pulse. In brief, the diffusion coefficient is determined by measuring the intensity decay of a Fourier transform starting at the center of the echo, the echo attenuation, as a function of the strength (g) or duration (δ) of the gradient pulse. With a few approximations, the echo

attenuation can be described by

$$I(k) = I_0 e^{-kD} \quad (3)$$

where I_0 is the echo intensity in the absence of gradient; $k = (\gamma\delta g)^2(\Delta - \delta/3)$, where γ is the proton magnetogyric ratio; D is the self-diffusion coefficient; and g , δ , and Δ are as defined above. In the stimulated echo sequence, which is used alternatively to the Hahn echo in spin systems with short T_2 values, three 90° rf pulses are used, and the field gradient pulses are switched on before the second and after the third rf pulse.^{32,33}

The measurements were done in a Bruker DMX200 spectrometer, operating at a ^1H resonance frequency of 200 MHz, with a gradient probe providing a maximum field gradient of 9 T/m. For the monitoring of the water self-diffusion, the basic Hahn echo pulse sequence was used. The surfactant self-diffusion was measured by the stimulated echo pulse sequence.

3. Results and Discussion

3.1. Phase Behavior. The phase behavior for the different bile salt–water systems was investigated and determined by a combination of visual inspection between crossed polaroids, polarizing microscopy, NMR methods, and SAXS data. The bile acid salts consist of the free salt SDC, the taurine conjugates STC, STDC, and STDCDC, and the glycine conjugate SGDC. Both isothermal and isoplethal methods were used to delineate phase boundaries, with an accuracy not better than 2–3 wt %. In a previous work,²⁶ lyotropic liquid-crystal behavior was reported for the bile salt STDC, at room temperature, and no further investigations have been carried out since then. In the current work, a global inspection of the phase diagrams in Figure 2a–e, for temperatures ranging between 5 and 40°C , shows that (i) the formation of liquid crystals by bile salts is a typical phenomena and (ii) there is a common pattern for this lyotropic phase behavior. Three single-phase regions as a function of concentration can be identified in Figures 2a–e: an isotropic (micellar) solution phase, an anisotropic liquid-crystalline phase, and a region with hydrated crystals. There are some noticeable differences between the salts, namely, in (i) the range of existence of the lc phase in the phase diagram, (ii) the phase equilibria in two-phase regions, and (iii) the kinetics of phase formation.

STC and STDC show well-defined phase boundaries, with occurrence of single- and two-phase regions (Figure 2a and 2b). For STC, at room temperature, samples within the range of 60–70 wt % display a monochromatic weak birefringence when viewed between crossed polaroids, and thus, they were assigned to the aniso lc region (Figure 2a). The two-phase region between the isotropic solution and the lc phase has some remarkable features. Some samples appear as cloudy and are taken to be a dispersion of the lc phase in the isotropic solution, i.e., the “proper” two-phase region. In some other samples, there is an isotropic solution and a weakly anisotropic upper phase, which only forms after a few days. From this phase, spherulitic crystals (with a characteristic macroscopic 4-fold symmetry) grow with time and eventually sediment at the bottom of the sample vial. Also, from the bottom phase, anisotropic needles appear coming up into the upper phase. This peculiar coexistence of spherulitic crystals with solution or birefringent phases, was previously reported by us for the STDC²⁶ and is also seen in the STC system. As will be shown below, some attempts were made to characterize structurally the spherulites by optical microscopy. In both the STC and STDC systems, there is complete disappearance of the anisotropic optical texture at temperatures slightly below 35°C . From all the

(29) Khan, A.; Fontell, K.; Lindblom, G.; Lindman, B. *J. Phys. Chem.* **1982**, *86*, 4266.

(30) Marques, E.; Khan, A.; Miguel, M. G.; Lindman, B. *J. Phys. Chem.* **1993**, *97*, 4729.

(31) Lindman, B.; Olsson, U.; Söderman, O. Surfactant solutions: aggregation phenomena and microheterogeneity. In *Dynamics of Solutions and Fluid Mixtures by NMR*; Delpuech, J.-J., Ed.; John Wiley & Sons: New York, 1995.

(32) Stilbs, P. *Prog. Nucl. Magn. Reson. Spectrosc.* **1987**, *19*, 1.

(33) Price, W. S. *Concepts Magn. Res.* **1997**, *9*, 299.

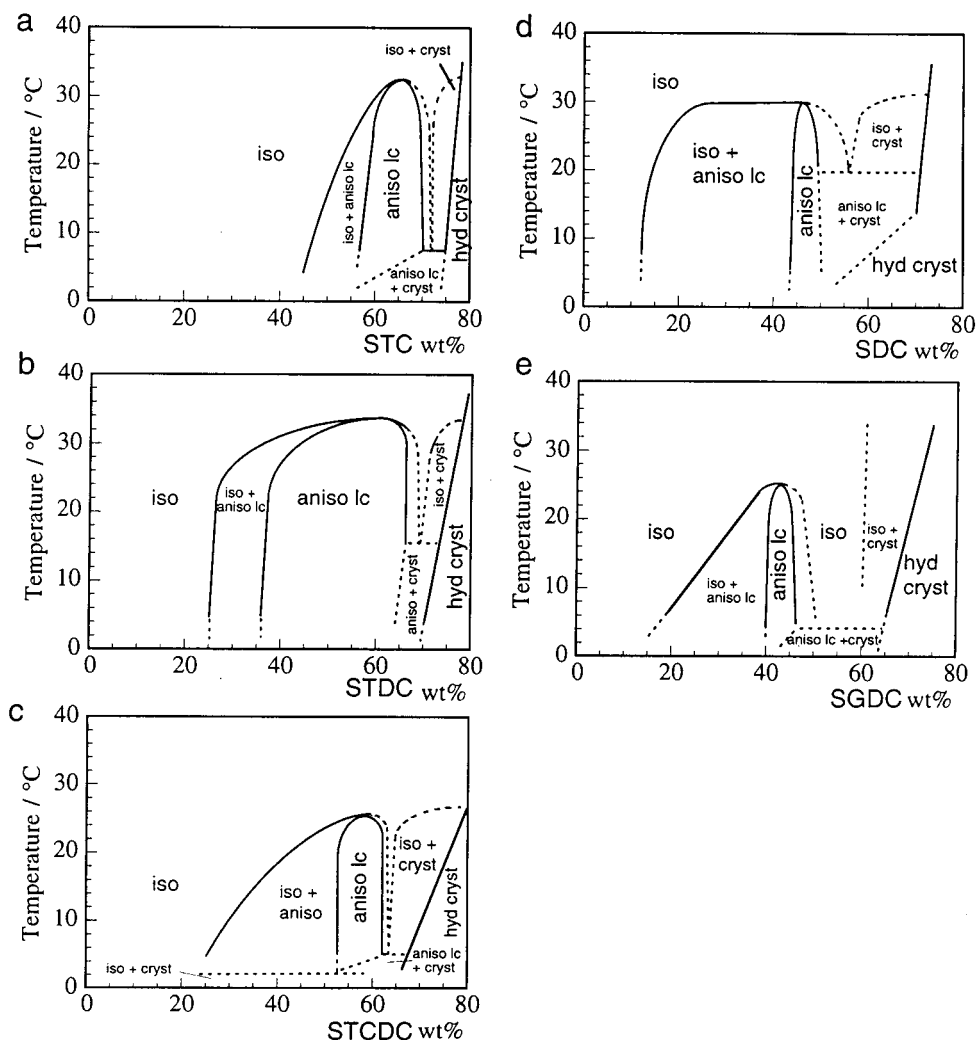


Figure 2. Phase diagrams for the different bile salt-water systems investigated here: (a) STC, (b) STDC, (c) STDCD, (d) SDC, and (e) SGDC. Notations are: iso, isotropic solution; aniso lc, anisotropic liquid crystal; cryst, crystals; and hyd cryst, hydrated crystals.

investigated systems, the STDC one shows the widest lc phase in terms of concentration range.

The STDCD salt shows the occurrence of a narrower liquid-crystalline region than the two previous systems (Figure 2b). The upper phase-transition temperature of the phase is about 25 °C (Figure 2c). At room temperature, a sample at 39.5 wt % shows small spherulitic crystals on the bottom, with a weak 4-fold symmetry, while the rest of the sample is isotropic. A sample at 44.3 wt % has small spherulitic crystals in a cloudy anisotropic matrix. At 49.6 wt %, no spherulitic crystals can be seen, and the sample is very cloudy. The last two samples are both transparent at visual observation and anisotropic through polarized light. At 55.5 wt %, the sample is birefringent and glitters, whereas a sample at 60.4 wt % has a weaker anisotropy. This typical sequence of observations allowed us to make a preliminary delineation of phase boundaries. For both the STC and STDC systems, the formation of spherulitic crystals in the biphasic region is not as clear (or even spectacular) as for STDC, but it can be seen at lower temperatures.

SDC and SGDC show a slightly more complex phase behavior. The lc region is quite narrow in the concentration range (about 5 wt %) in both systems. A wide two-phase region between the isotropic solution and the lc phase is present for SDC (Figure 2d). The region where optical anisotropic textures are clearly evident between crossed

polaroids is almost always a two-phase region (iso/aniso or aniso/cryst) in the time span of a week. Within only a few weeks, single-phase anisotropic samples are formed. Similar observations are made for SGDC. In this system, the liquid crystal slowly appears from biphasic solution-crystal samples. It is clear that in the two systems the kinetics of liquid-crystal formation is considerably slow, and much slower than that for the previous systems. Above around 32 °C for SDC and 28 °C for SGDC, the lc phase melts totally onto the isotropic solution.

Several relevant comments are to be made. First, the depiction of the two-phase region between the micellar solution and the liquid crystal as *iso-aniso lc* in Figure 2a–e does not convey the complete picture of the phase behavior. In view of what was described above, the formation of spherulitic crystals is a general phenomena. These structures can either be ascribed to a metastable liquid crystal or to transient nucleation sites for the formation of the aniso lc phase. Second, the isotropic phase beyond the lc phase is depicted as being identical to the isotropic micellar phase. In most systems, one finds that this isotropic viscous phase (flowing under gravity) occurs in equilibrium with crystals. For the case of SGDC, however, it was possible to detect a single isotropic phase between the aniso lc and the hydrated crystals. The samples are isotropic and rather stiff and clearly resemble a cubic liquid-crystalline phase more than a viscous

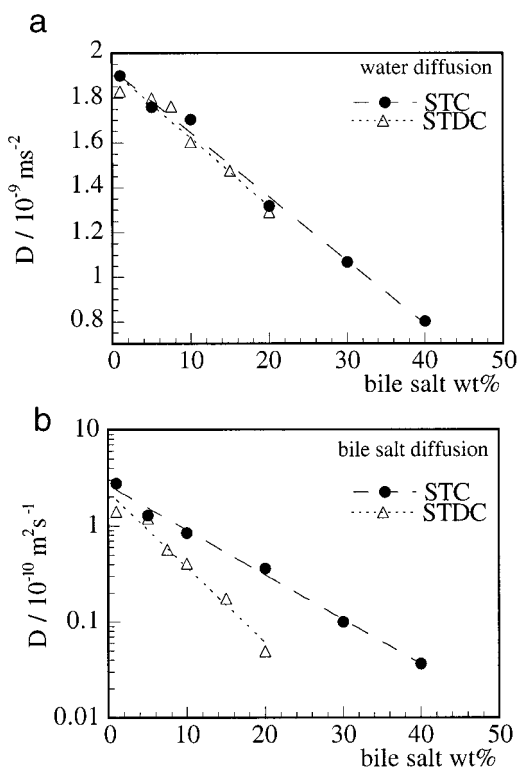


Figure 3. Self-diffusion measurements in the isotropic solution of STC and STDC at 25 °C: (a) water diffusion; (b) bile salt diffusion. The lines are guides for the eyes.

solution. Therefore, the possibility of there being an isotropic phase distinct from the isotropic micellar solution at very high surfactant concentration cannot be excluded.

3.2. NMR Self-Diffusion Study of the Isotropic Solution Phase. A structural study of the isotropic solution of the bile salts was performed by means of NMR self-diffusion measurements, for the STC and STDC systems. These two molecules are representative of trihydroxy and dihydroxy salts, respectively, and allow an illustration of the relation between molecular structure and aggregate growth. Both the water (Figure 3a) and the bile salt (Figure 3b) diffusion were measured. It is known that the magnitude of the obstruction effect to solvent diffusion is critically dependent on the size, shape, and concentration of aggregates.³⁴ Thus, spherical and rodlike micelles give rise to minor obstruction effects, whereas disklike and oblate micelles cause larger effects. In Figure 3a, no significant differences can be seen between the two systems in the reduction of the water diffusion coefficient (D) values as a function of concentration. The simplest interpretation for these results would be that, as the concentration rises, a similar growth of the aggregates occurs in both systems and the aggregates should bear similar shape.

However, the surfactant diffusion shows marked differences between the two systems (Figure 3b). It must be recalled here that at surfactant concentrations equal and above roughly $50 \times \text{cmc}$, the monomer contribution to the measured surfactant diffusion coefficient is negligible. Consequently, the surfactant diffusion is virtually identical to the micellar diffusion, i.e., $D_{\text{surf}} \approx D_{\text{mic}}$. As the surfactant concentration further increases, the latter assumption is no longer valid since interaggregate obstructions must be taken into account.³¹ It can be seen in

Figure 3b that for STDC solutions, the D_{surf} values are always smaller than those for STC, at the same concentration. Moreover, the decrease in D_{surf} with concentration is more pronounced for STDC than for STC. A rough estimation of the aggregate hydrodynamic radius can be made from the measured D_{surf} values, through the simple Stokes–Einstein equation (discarding the correction for interparticle obstructions). This can be done, for example, at 20.0 wt %, a concentration well above the cmc of both molecules (ca. 0.08 and 0.2 wt % for STDC and STC, respectively, at 25 °C).² D_{surf} for STDC has a value of $5.0 \times 10^{-12} \text{ m}^2 \text{ s}^{-1}$, corresponding to a hydrodynamic radius R_{H} of 390 Å. At the same STC concentration, D_{surf} is $3.6 \times 10^{-11} \text{ m}^2 \text{ s}^{-1}$ which gives $R_{\text{H}} = 54 \text{ Å}$, a value 7 times smaller than that for STDC. Since there is a close similarity in structure between the two molecules, the surfactant diffusion results indicate a more pronounced aggregate growth with surfactant concentration for STDC than that for STC. As for the water self-diffusion results, a simple rationalization can be done. Larger aggregates for STDC, at identical bulk concentration to STC, imply a smaller concentration of aggregates. However, the solvent obstruction effect is relatively insensitive to the particle volume fraction, unless the shape of the particles is very different.³⁴ Thus, the differences in size and shape between the STC and STDC micelles cannot be “sensed” by water self-diffusion, and a comparable decrease in the solvent diffusion coefficients with surfactant concentration is observed.

The diffusion results presented here are compatible with the literature reports regarding aggregation numbers for the micelles of tri- and dihydroxy bile salts and micellar growth. Mazer et al. have shown that sodium cholate forms smaller micelles than the deoxy- and chenodeoxycholate derivatives.⁷ It has been reported that, upon addition of electrolyte (NaCl), STDC shows a much more pronounced micellar growth than STC.^{2,35} The reason for these differences in micellar growth obviously lie in the presence of the additional OH group in the trihydroxy salts. Since the dihydroxy molecule has one less hydrophilic group, the polar face of its steroid ring is more hydrophobic, and this will have large implications in the packing of the molecules. The gain in interfacial free energy per molecule associated with self-aggregation is larger for the dihydroxy; therefore, from this point of view, the formation of larger micelles should be favored from start. It should be noted that the packing of di- and trihydroxy bile salts in neat and in mixed micelles with several surfactants seems to be reasonably complex and concentration-dependent.¹⁷

The packing has been viewed in terms of a preference for a perpendicular or a flat positioning with regard to the polar–apolar interface for di- and trihydroxy salts, respectively.⁷ Besides the hydrophobic back-to-back interactions, intermolecular hydrogen bonding has also been proposed to occur in the aggregate formation.^{2,17} It is also relevant to mention that the self-diffusion results presented here for STC and STDC are coherent with the phase behavior observations made in the previous section. If the STDC micelles are bigger and grow faster with concentration, then the formation of the lc phase should occur for smaller concentrations than those for STC. This is indeed observed in the phase diagrams in Figure 2a,b.

3.3. Liquid-Crystal Formation. A. Polarizing Microscopy. In most surfactant systems, polarizing microscopy is invaluable in the detection of anisotropic liquid crystals and their assignment. Anisotropic optical textures

(34) Jönsson, B.; Wennerström, H.; Nilsson, P.-G.; Linse, P. *Colloid Polym. Sci.* **1986**, *264*, 77.

(35) D’Archivio, A. A.; Galantini, L.; Gavuzzo, E.; Giglio, E.; Scaramuzza, L. *Langmuir* **1996**, *12*, 4660.

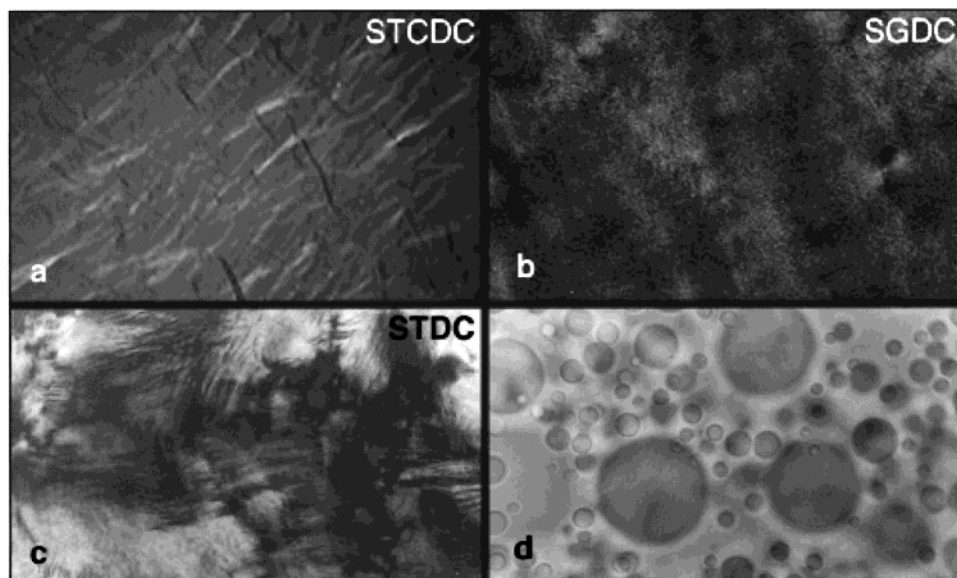


Figure 4. Liquid-crystalline textures in bile salt-water systems as seen in the polarizing microscope: (a) 57.5 wt % STCDC, at 22 °C; (b) 42.5 wt % SGDC, at 22 °C; (c) 40.0 wt % STDC, at 22 °C; and (d) 40.0 wt % STDC, when heated to 40 °C, showing droplets in an isotropic medium (under normal light). Magnification: 200 \times .

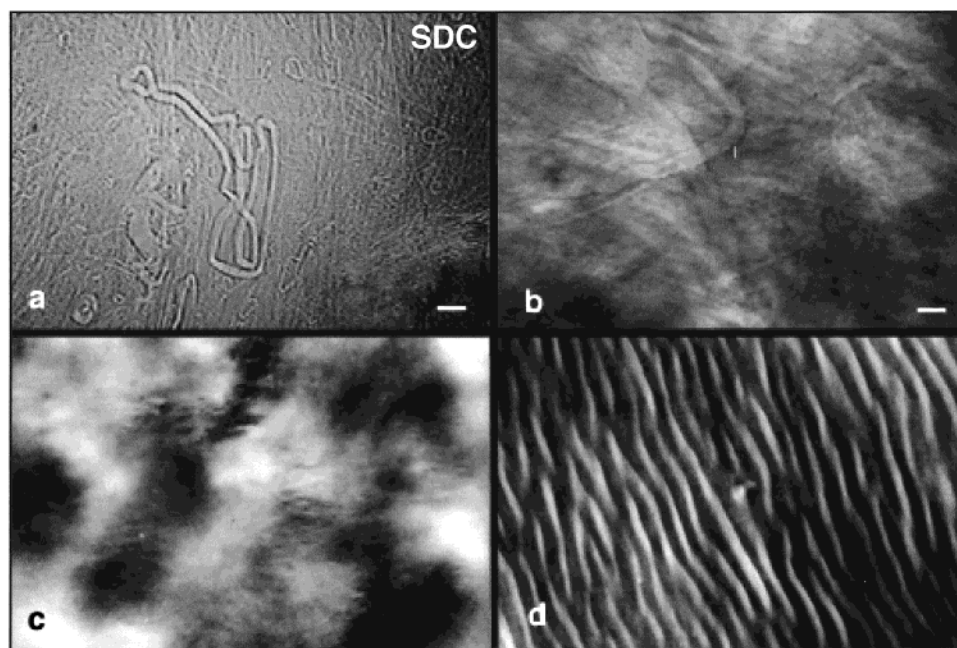


Figure 5. Polarizing microscopy observations for the SDC–water system at 22 °C: (a) and (b) Giant fibers and anisotropic liquid-crystalline domains at 26.6 wt % SDC, in the two-phase region isotropic solution plus spherulitic crystals. (c) and (d) Anisotropic liquid-crystalline phase for 47.1 wt % SDC. Magnification: 200 \times . Bar in parts a and b is 40 μm .

were observed for the liquid-crystalline samples in all binary systems, with the exception of STC. All the textures in Figure 4a–c belong to the hexagonal type. The most well-defined textures appear for STCDC (Figure 4a), where birefringent domains similar to hexagonal battonnets appear, and for STDC (Figure 4c), where a clear striated nongeometric texture appears.^{27–29} For SGDC, a very weakly birefringent, somewhat ill-defined texture was detected (Figure 4b) of the nongeometric, nonstriated type. When STDC samples displaying the texture in Figure 4c at room temperature are heated above 35 °C, the liquid crystal melts, and in the glass slide, droplets of an optically isotropic phase can be seen (Figure 4d).

Attempts were made to separate the spherulitic crystals occurring in biphasic samples and observe them between slide and cover-slip in the polarizing microscope. A sample

at a composition of 26.6 wt % in the SDC system was selected. The bottom phase was separated from the isotropic solution and viewed in the microscope (Figure 5a and 5b), showing some remarkable features. Giant fiberlike structures can be seen throughout the sample (the bar in Figure 5a,b corresponds to 40 μm), forming a very dense material. In some areas of the sample, domains of nongeometric, nonstriated texture are seen mixed with the fiberlike structures (Figure 5b). In a single-phase sample within the lc region, at 47.1 wt % SDC, the anisotropic nongeometric texture is visible. Another interesting feature of this system is that by applying a small pressure onto the cover-slip, a well-defined undulating structure of the type imaged in Figure 5d is observed. The long rodlike structures observed in Figure 5a,b appear to be in line with the helical-based hydrated fibers first

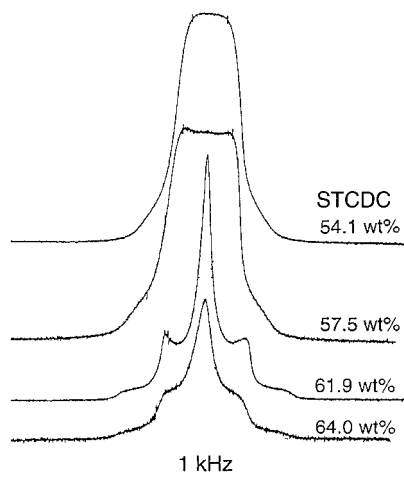


Figure 6. ^2H NMR spectra for the system STCDC–water, at 5 °C.

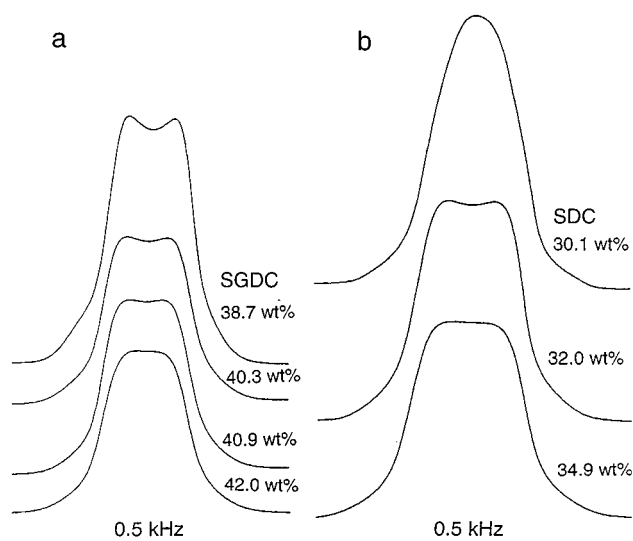


Figure 7. ^2H NMR spectra for the systems (a) SGDC–water and (b) SDC–water, at 7.5 °C.

reported by Blow and Rich a few decades ago^{9,10} and more recently investigated by Giglio et al.¹¹ and Briganti and co-workers.¹² One can speculate if the structure of the liquid-crystalline phase is directly related with a positional and orientational arrangement of these rodlike structures to yield anisotropy.

B. ^2H Quadrupolar Splitting NMR. A general observation borne out from the ^2H NMR study was that ^2H splittings could be detected for the aniso lc phase in several binary systems. The splitting occurs more frequently with superimposed isotropic signals in the biphasic regions. In fact, for most samples in the lc phase of the different bile systems, the water deuteron signal consists of a very broad signal. A representative collection of ^2H spectra is shown for STCDC in Figure 6, recorded at a temperature of 5 °C. At 54 wt % of STCDC within the lc phase, a broad signal (≈ 0.7 kHz) is recorded, whereas at 57.5 wt%, a splitting is present. As the concentration increases toward the two-phase region, a singlet and a clear splitting are observed, indicating a two-phase region of isotropic phase and anisotropic lc. In Figure 7a, for the SGDC system, it can be noted that a sample in the vicinity of the lc phase boundary (38.7 wt %) shows a splitting, while as the composition enters the lc phase the doublet is replaced with a broad signal. For SDC (Figure 7b), a splitting could only be detected in the biphasic region.

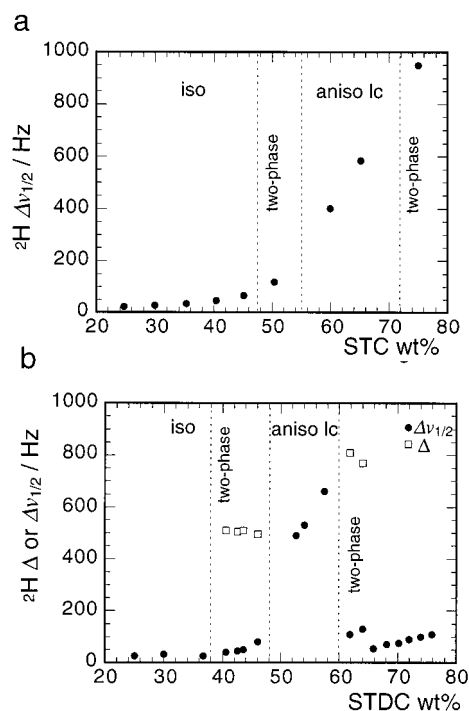


Figure 8. Deuterium splitting ($^2\text{H} \Delta$) or signal half-width ($^2\text{H} \Delta v_{1/2}$) vs bile salt weight percent for (a) STC, at 18 °C, and (b) STDC, at 12–13 °C.

The ^2H quadrupolar splitting for doublets or the half-width for single signals are plotted versus surfactant weight percent in parts a and b of Figure 8 for the STC and STCDC systems, respectively. For the STC–water system, no water ^2H splitting could be detected in single- or two-phase samples containing the liquid-crystalline phase, even after considerable sample aging (weeks). Samples in the lc phase showed as broad signals with Δ values of 0.4–1 kHz (Figure 8a). In the case of STCDC, for samples in the lc region or in biphasic regions in the vicinity of the lc phase, the spectra showed as a broad signal plus a small splitting on the order of 0.5–0.8 kHz (Figure 8b).

The ^2H NMR splittings are much smaller than those usually observed for typical liquid-crystalline phases in surfactant systems.^{36,37,30} This effect might result from very small values of the order parameter for the binding of water, indicating in turn a small degree of anisotropy for the liquid crystal. The nonappearance of ^2H splittings for anisotropic phases has been previously reported.³⁸ The broad signals observed are an indication that fast exchange conditions (between “free” and “bound” water) are not fulfilled, possibly resulting from the fact that the lc microcrystallites in the sample are not large enough (not even after weeks of undisturbed aging).

C. SAXS Measurements. Structural length scales in lyotropic liquid crystals are on the order of 10–500 Å, and thus, SAXS data can often be used to determine the type of liquid crystal present in a sample. Different liquid crystals (lamellar, hexagonal, cubic, etc.), possessing some type of long-range structural order, show well-defined Bragg peaks (*reflections*), resulting from the constructive interference of reflected X-rays. Theoretically, a hexagonal phase is built up of infinitely long cylindrical aggregates packed in a 2-D hexagonal array, with Bragg peak

(36) Tiddy, G. J. T. *Phys. Rep.* **1980**, *57*, 1.

(37) Kang, C.; Khan, A. J. *Colloid Interface Sci.* **1993**, *156*, 218.

(38) Khan, A.; Jönsson, B.; Wennerström, H. *J. Phys. Chem.* **1985**, *89*, 5180.

positions corresponding to

$$q_{hk} = \frac{2\pi(h^2 + k^2 + hk)^{1/2}}{d} \quad (4)$$

where q_{hk} is the scattering vector of the $[hk]$ reflection, h and k are the Miller indices, and d is the Bragg lattice spacing. In the hexagonal phase, $(h^2 + k^2 + hk)^{1/2}$ takes the values 1, $\sqrt{3}$, $\sqrt{4}$, $\sqrt{7}$, and $\sqrt{9}$, corresponding to the first five reflections $(hk) = (10)$, (11) , (20) , (21) , and (30) . The hexagonal cylinder radius r_c , in the normal hexagonal phase, can be calculated by

$$r_c = d \left(\frac{2f}{\pi\sqrt{3}} \right)^{1/2} \quad (5)$$

where f is the volume fraction of the nonpolar domains. The interfacial area per surfactant molecule a_s , also in the normal hexagonal phase, is obtained according to

$$a_s = \frac{2fv_s}{r_c\phi_s} \quad (6)$$

where v_s is the volume per surfactant molecule and ϕ_s is the volume fraction of surfactant. In the reverse hexagonal phase, f should be replaced with $1 - f$ (i.e., the volume fraction of polar domains) in eqs 5 and 6.

In a previous report for the STDC–water system, it was found that samples within the lc phase showed a diffraction pattern with peaks on the order of 1:1.73:1.89, thus with close similarity to the hexagonal diffraction pattern (1: $\sqrt{3}$:2: $\sqrt{7}$:3). In this work, a sample with STC at 60 wt %, lying in the lc phase region, shows a practically unequivocal hexagonal diffraction spectra up to fifth-order reflection, with peaks in the order 1:1.75:2.00:2.77:3.09 (Figure 9a). In other binary systems, patterns very close to a hexagonal one could be identified, but only for samples in biphasic regions containing the anisotropic lc phase. This is the case shown in Figure 9b for STCDC, at 44 wt %, where four correlation peaks in the order 1:1.76:2.00:2.66 are seen. For SDC, at a composition of 39.1 wt % in the close vicinity of the lc boundary, a pattern with the peak order 1:1.71:2.00:2.69 can also be identified.

All the SAXS data clearly points to a hexagonal-type liquid crystal formed by the bile salts here investigated, entirely consistent with the characteristic optical textures in Figures 4 and 5. However, this phase is most probably built up of aggregates not of a conventional type. It is likely that such aggregates bear a close structural connection with the long rodlike aggregates (or fibers) that have been drawn from concentrated isotropic solutions and for which a helical structure has been proposed.^{9,10,12–14} Bearing in mind the latter results and from the location of the lc phase in the phase diagram, we tentatively assign this phase to a reverse-type of hexagonal phase. Under this assumption, the SAXS results obtained for the representative samples in Figure 9 were analyzed and are shown in Table 1. The calculated lattice parameters in Table 1 include the lattice spacing d , the lattice parameter α (nearest-neighbor distance, $\alpha = 2d/\sqrt{3}$) and the hexagonal cylinder radius r_c . In these calculations, $v_s = 530 \text{ \AA}^3$ was used,² it was assumed that $f \approx \phi_s$, and consistently with the proposed reverse structure, the factor $(1 - f)$ was used in eqs 5 and 6. The structural parameters listed are to be taken on a semiquantitative basis, in view of the approximations made. Nonetheless, they allow us a qualitative fruitful discussion of trends. From Table 1, it can be seen that STC has the smallest cylinder radius and the largest interfacial area per molecule (65 \AA^2). This

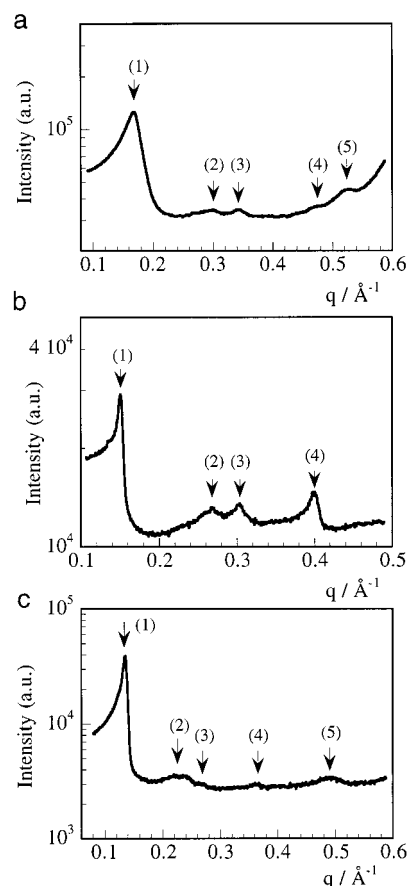


Figure 9. Slit-smear SAXS patterns for bile salt-water samples: (a) 59.9 wt % STC, at 22 °C; (b) 43.6 wt % STCDC, at 15 °C; (c) 39.1 wt % SDC, at 22 °C. The numbers indicate the n th order correlation peak ascribed to a hexagonal lattice.

is in agreement with the fact that this salt has three hydroxy groups and thus is the least hydrophobic of the series. STCDC has a larger value of a_s than STDC and SDC, and this fact can be rationalized as follows: with the two OH groups in carbons 3 and 7 (cf. Figure 1b), STCDC cannot pack in the interface as tightly as STDC and SDC (OH groups in carbons 3 and 12). The observed trend in a_s , STC > STCDC > SDC > STDC, is thus essentially consistent with the solubility sequence of the salts, as discussed below.

4. Summary

It has been shown that all the investigated bile salt molecules form an anisotropic liquid-crystalline phase in water, between the isotropic solution and the hydrated crystals. This pattern of lyotropic behavior appears to be the general case for bile salts. A broad rationalization of the observed phase behavior can be done on the basis of the known solubility of the salts, in turn dependent on their chemical structure.² The trihydroxy salts are more soluble than the dihydroxy ones. The taurine and glycine conjugates are much more soluble than the free salts due to their peptide bonds and strong ionic groups, and the taurine is slightly more soluble than the glycine due to its higher polarity. The chenodeoxy derivatives are slightly more soluble than the deoxy ones. All these observations are reflected in the obtained cmcs for different salts of the same alkali metal ion.² Accordingly, the maximum solubility for the salts studied here follows the order STC > STCDC > STDC > SGDC > SDC (i.e., the “hydrophilicity” of the salts decreases in this order). From the phase

Table 1. Results for SAXS Measurements in Liquid-Crystalline Samples of Different Bile Salt-Water Systems

bile salt	wt %	d^a (Å)	a^b (Å)	r_c^c (Å)	a_s^d (Å ²)	$q_1^{e(10)}$ (Å ⁻¹)	$q_2(11)$ (Å ⁻¹)	$q_3(20)$ (Å ⁻¹)	$q_4(21)$ (Å ⁻¹)	$q_5(30)$ (Å ⁻¹)
STC	59.9	37.0	42.7	16.3	65.0	0.170	0.297	0.340	0.472	0.526
STDC ^f	40.0	51.5	59.5	26.3	40.3	0.122	0.210	0.231		
STCDC	43.6	41.9	48.4	20.9	50.6	0.150	0.265	0.303	0.400	
SDC	39.1	46.9	54.2	23.4	45.3	0.134	0.229	0.270	0.361	0.490

^a Lattice spacing, obtained from the (10) reflection. ^b Lattice parameter (nearest-neighbor distance). ^c Hexagonal cylinder radius. ^d Interfacial area per surfactant molecule. ^e q_n is the q value for the n th order (hk) reflection. ^f Values from Edlund et al.²⁶

diagrams in Figure 2, it can be seen that, at 20 °C, the solubility order is STC > STCDC ≥ SGDC > STDC > SDC, which is not far from the expected one. For example, at 20 °C, the solubilities in bile molar fraction for STC and STDC is 0.036 and 0.011, respectively, indicating the large effect on solubility of the additional OH group.

The observed thermal stability of the lc phase for the bile salts is small compared to those of typical ionic surfactants. This fact suggests weak energy differences between the isotropic solution and the liquid crystal. The thermal stability of a liquid-crystalline phase is expected to increase with an increasing hydrophilic character of the surfactant headgroup (for identical hydrophobicity). For instance, phase-behavior studies on sodium and potassium surfactants show a relative hydrophilicity for anionic groups corresponding to carboxylate >> sulfonate > sulfate.³⁹ The comparison between the phase diagrams of SDC, SGDC, and STDC (which differ only in headgroup composition) in Figure 2 does not show significant differences in thermal stability, but the taurine salt (the most hydrophilic) is indeed slightly more stable than the glycine and the free salts. When comparing the mole fraction of bile salt for the lower limit of the lc phase, one has 0.033, 0.025, and 0.019 for SDC, SGDC and STDC, respectively. Moreover, the width of the lc phase in composition has the order STDC >> SGDC ≈ SDC. Solely on the basis of these observations, it appears that the increasing hydrophilicity of the headgroup favors the formation of the lc phase. The effect on phase behavior of the number and position of OH groups is considerable, in view of the phase diagrams for the STC, STDC, and STCDC systems. In particular, changing the OH group from the αC-12 to the αC-7 position on going from the deoxy to the chenodeoxy salt, respectively, brings about a lower thermal and compositional stability for the lc phase. What appears to be borne out from the phase diagram observations is that chemical structure plays a relatively intricate role in the aggregation behavior of bile salts. This is not surprising, since both hydrophobic back-to-back interactions and intermolecular hydrogen bonds are proposed to take place in the self-assembly of the molecules.

The kinetics of phase transformation is different for the different bile acid salts. For instance, birefringent structures form in 1–2 days in the STDC–water system, while much longer times, up to months, are required for the other salts. The very long time required to have equilibrium structures is an indication that the difference in stability between the different states of organization for bile acid salts is small. Some unusual phase-transition phenomena are observed. There is slow formation of anisotropic textures from the corresponding dispersed solids and occurrence, for some salts, of transient spherulitic domains. These uncommon nucleation effects, the

long equilibration times and the puzzling temporal sequence of the transformations, may have led most authors in the past to discard *tout court* the occurrence of liquid-crystalline phases in such systems.

The optical textures, the SAXS data, and the ²H NMR spectra taken in combination point to an anisotropic liquid-crystalline phase of hexagonal symmetry. This phase is most probably built up of nonconventional micellar-like aggregates of the reverse type. The SAXS spectra were analyzed under this assumption, and some reasonable trends were identified. The possibility of a close structural relation between this hexagonal phase and the long rodlike aggregates of helical structure, previously described for the isotropic phase,^{12–14} has to be kept in mind. The solutions observed at concentrations of bile acid salt higher than those of the lc phase are extremely viscous, and it is not easy to ascertain whether they are true solutions or cubic phases. A more detailed study of this viscous isotropic phase is required.

Lytotropic liquid crystals formed by surfactants such as soaps, detergents, and lipids, are considered to require a liquidlike state of the flexible chains as a prerequisite for their assembly. Obviously this does not hold for molecules with rigid ring structures which nonetheless bear lyotropic properties. There is indeed a vast class of molecules, termed *chromonic* materials and including drugs, dyes, and antibiotics, which show the occurrence of lyotropic liquid crystals such as nematic and hexagonal phases (cf. recent review by Lydon⁴⁰). Such molecules do not have surface activity, they do not possess flexible aliphatic chains since they are usually based on aromatic ring structures, and they often have polar groups around the peripheries of the ring structure (implying that polar and apolar regions are not clearly separated). There is thus some structural analogy between the bile salts and such molecules. Concomitantly, in terms of lyotropic behavior, bile salts can be seen as lying in an intermediate position between the chromonic materials and the common flexible chain surfactants. It must be borne in mind that liquid-crystal formation does not necessarily imply any particular state of the molecule but rather a positional order of domains. In this context, it is not at all surprising that the bile acid salts, which form supramolecular aggregates of certain complexity in solution (*viz.* fiberlike structures), can also form liquid-crystalline phases.

Acknowledgment. The Swedish Research Council for Engineering Sciences (TFR) and PRAXIS XXI, Portugal (Project 2/2.1/QUI/411/94) are gratefully acknowledged for financial support. H.E. gratefully acknowledges STINT (The Swedish Foundation for International Cooperation in Research and Higher Education), for a Postdoctoral Scholarship in the Department of Chemical Engineering, University of Delaware.

LA9912803

(39) Laughlin, R. G. *The Aqueous Phase Behavior of Surfactants*; Academic Press: San Diego, 1994.

(40) Lydon, J. *Curr. Opin. Colloid Interface Sci.* **1998**, *3*, 455.